JOURNAL OF GEOPHYSICAL RESEARCH, VOL. 103, NO. D6, PAGES 6189–6202, MARCH 27, 1998

Ground-based spectroscopic observations of atmospheric ozone from 142 to 359 GHz in southern Europe

Juan R. Pardo[1]
NASA Goddard Institute for Space Studies, New York City

José Cernicharo
Consejo Superior de Investigaciones Científicas, IEM, Madrid

Laurent Pagani
DEMIRM, URA336 du CNRS, Observatoire de Paris-Meudon, Paris

Abstract. During different periods of time between 1991 and 1996 we have achieved ground-based observations of rotational lines of atmospheric ozone using two different ground-based radio telescopes located in southern Europe: the 30 meters IRAM radio telescope at Pico Veleta (latitude 37:04:05.60°N, longitude 3:23:58.10°W, altitude 2850 m) and POM-2 at Platcau dc Burc, (Hautcs Alpcs, France, latitude 44:38:02.00°N, longitude 5:54:28.50°E, altitude 2550 m). A total of eight different ozone lines have been observed with frequencies in the range 142-359 GHz. Several back-end spectrometers were able to analyze the incoming signal with very different frequency resolutions and total spectral coverage. This has allowed us to retrieve information about the vertical profile of ozone over a relatively wide range of altitudes. The retrieval itself has been achieved by means of a nonlinear least squares fit of the observed line profile, taking into account the spectroscopic, observational, and instrumental parameters of the different observations. A comparison between the ozone amounts retrieved from observations of different ozone lines in winter and summertime is given separately. Ozone amounts obtained from the different instruments and ozone lines are consistent.

1. Introduction

The importance of ozone on the absorption of solar UV radiation which governs the temperature profile of the stratosphere is well known. This profile depends on a very complicated dynamical and chemical system that is presently under study. The monitoring of O_3 and other minor (chemically related) gases is now of great interest for problems like the depletion of ozone on a global scale and the destruction of ozone in the lower stratosphere over Antarctica.

Ground-based spectroscopic observations of minor atmospheric gases at millimeter wavelengths have been carried out by different groups during the last years (for O_3, see, for example, Lobsiger and Künzi [1986], Zommerfelds *et al.* [1989], Ricaud *et al.* [1991], Connor *et al.* [1994], and Tsou *et al.* [1995]; for stratospheric/mesospheric H_2O, see Bevilacqua *et al.* [1987], Tsou *et al.* [1988], Nedoluha *et al.* [1995], and Pardo *et al.* [1996]; for ClO, see de Zafra *et al.* [1995]). Ground-based spectroscopic measurements at millimeter wavelengths have been shown as a useful technique because they do not depend on sunlight and are not significantly affected by aerosols. They also help to validate satellite data sets. Such an observation technique has also the advantages of a relative wide range of altitude coverage and a low cost compared with satellite observations. Some disadvantages of the technique are the restricted local meaning of the data and a vertical resolution limited to about the value of the pressure scale height (~10 km or so; see explanation below). At some frequencies there is also the problem (specially out of the polar regions) of absorption of the stratospheric signal by tropospheric water vapor, partially solvable by placing the detectors in high mountain sites. The limited vertical resolution comes from the fact of the ill-posed nature

[1]Also at DEMIRM, URA336 du CNRS, Observatoire de Paris-Meudon, Paris, and Observatorio Astronómico Nacional, Madrid.

Paper number 97JD03628.
0148-0227/98/97JD-03628$09.00.

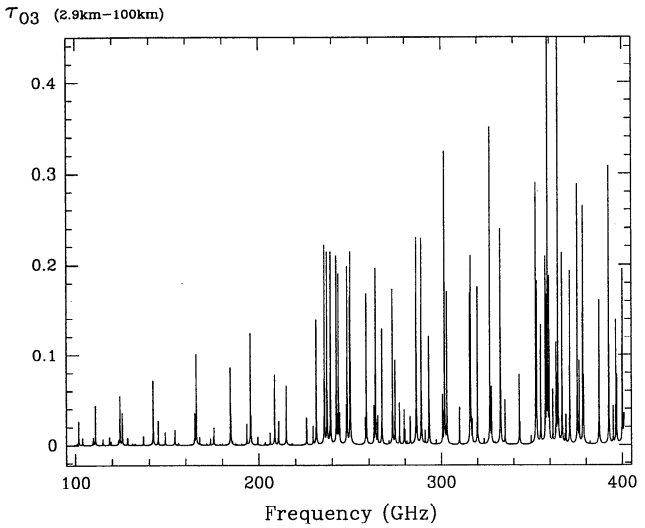

Figure 1. Integrated ozone opacity from 2.9 km to 100 km as a function of frequency calculated by the Atmospheric Transmission at Microwaves (ATM) model for the standard vertical profile of ozone given in the U.S. Standard, 1976, midlatitude winter atmosphere.

of the inversion problem. It means that only a few altitude-averaged values of the mixing ratio corresponding to the observed gas can be retrieved.

Retrieval algorithms of atmospheric parameters from this kind of observation usually involve a linear approach (as, for example, the Backus-Gilbert method [see Bevilacqua and Olivero, 1988; and Backus and Gilbert, 1970], the optimal estimation linear constrained method [Rodgers, 1990], and the method by Chahine-Twomey [Twomey, 1997]). They are also usually developed for a particular instrument and a particular resonance. In this work we use a general nonlinear least squares fit algorithm for spectroscopic observations (ground based as well as satellite) of minor atmospheric gases in the frequency region 10-1000 GHz. The retrieval is based on the forward atmospheric radiative transfer code ATM [Cernicharo, 1988; see also Pardo, 1996] which is actually used in a large number of European millimeter wave radio telescopes to estimate the atmospheric opacity for astrophysical observations.

Ozone has a very rich rotational spectrum in its fundamental vibrational state [see Gordy and Cook, 1984] (Figure 1 of this paper) because it is an asymmetric rotor. In the frequency range 10-1000 GHz, O_3 is the third-most important molecule contributing to the Earth's atmospheric line spectrum (after O_2 and H_2O; see Pardo [1996]). Observed from the ground, brightness temperatures of some O_3 lines are as high as a few tens of Kelvin degrees under clear sky conditions and ~1 to 2 mm of integrated water vapor above the site. These lines appear above a continuum whose level fluctuation depends almost exclusively on the tropospheric H_2O (the amount of O_2 is much more stable). The lines we have observed are located between strong atmospheric lines of H_2O (centered at 183, 325, and 380 GHz) and O_2 (at 119 and 368.5 GHz). Table 1 shows spectroscopic parameters [from Rosenkranz, 1992; Pardo, 1996] of the eight O_3 lines reported in this paper.

Most ground-based O_3 observation campaigns have selected ozone resonances below 150 GHz (i.e., Tsou *et al.* [1995], and Ricaud *et al.* [1991] used the $6_{1,5} \rightarrow 6_{0,6}$ ozone transition centered at 110.836 GHz, whereas Lobsiger and Künzi [1986] and Zommerfelds *et al.* [1989], observed the $5_{1,5} \rightarrow 4_{0,4}$ line at 142.175 GHz). The main reason for this is the increase of tropospheric water vapor absorption with frequency. On the other hand, ozone lines appear stronger with increasing frequencies.

The intent of this work has been to demonstrate the possibility of obtaining useful ozone data with the radio telescopes POM-2 (Plateau de Bure, French Alps) and IRAM-30 m (Sierra Nevada, Spain) at higher frequencies than have been used to date. The paper gives

Table 1. Spectroscopic Parameters of O_3 Rotational Resonances Reported in This Work

$J_{K_a\ K_b}$	$J'_{K'_a\ K'_b}$	ν, GHz	Line Strength[a]	E_{lower}, K	$\Delta\nu_0$, MHz/mbar	Temperature Exponent, x
$10_{1\ 9}$	$10_{0\ 10}$	142.17510	8.27	66.1	2.50	0.70
$5_{1\ 5}$	$4_{0\ 4}$	208.64242	3.07	12.1	2.41	0.76
$16_{1\ 15}$	$16_{0\ 16}$	231.28151	9.02	161.9	2.30	0.76
$14_{2\ 12}$	$14_{1\ 13}$	237.14613	10.9	134.8	2.30	0.76
$18_{2\ 16}$	$18_{1\ 17}$	239.09326	14.9	216.1	2.28	0.76
$12_{2\ 10}$	$12_{1\ 11}$	242.31869	8.77	101.4	2.31	0.76
$30_{3\ 27}$	$30_{2\ 28}$	358.19981	24.0	591.5	2.30	0.76
$16_{0\ 16}$	$15_{1\ 15}$	358.85334	11.2	144.7	2.25	0.76

These lines are placed in the tropospheric windows accessible from the ground between the 119 and 368 GHz O_2 resonances and the 183 and 325 GHz H_2O resonances.

[a]The line strength is a nondimensional number related to the transition dipole matrix element [e.g., Gordy and Cook, 1984] which gives, together with the energy of the lower level of the transition (E_{lower}), an indication of the relative line intensities. J, K_a K_b are rotational quantum numbers used to describe the rotational energy levels of an asymmetric top molecule [see also Gordy and Cook, 1984]. $\Delta\nu_0$ and x were introduced in equation (6).

information on O_3 lines never used to date to monitor O_3 and could help in planning future ozone monitoring campaigns. It is our intention in the future to keep the POM-2 instrument devoted to O_3 monitoring above 200 GHz and to create an automatic procedure for atmospheric data acquisition on the IRAM-30 m telescope running simultaneously with the astrophysical observations.

We present in section 2 a description of the instruments and of the observations. Section 3 is devoted to a brief review of the theory involved in the atmospheric inverse radiative transfer problem for millimeter ground-based measurements and a presentation of the inversion code. Section 4 is devoted to the analysis of our measurements. A general discussion of the results is given in section 5, paying special attention to some particular cases. Summary and conclusions are given in section 6.

2. Instrumentation and Observations

The whole set of observations we present in this paper were taken between 1991 and 1996 using two ground-based radio telescopes. The main characteristics of these instruments appear in Table 2. A more detailed description follows.

The IRAM millimetric telescope (30 m of diameter) is located at Sierra Nevada, Spain, 2850 m above sea level. A summary of the characteristics of this telescope is given by Cernicharo [1988]. The observations carried out with this instrument, at different epochs, made use of two Supraconductor-Isolator-Supraconductor (SIS) receivers working at a wavelength of around 2 mm and 1.3 mm. An open structure SIS receiver at 350 GHz was also tuned at the frequencies of two ozone lines around 358 GHz. The receiver intermediate frequency in the IRAM-30 m system is 3.932 GHz. The spectrometers consisted of two (512 x 1 MHz and 256 x 100 kHz) filter banks. Taking into account the typical values of the collisional broadening parameters of millimetric O_3 lines (2 to 3 MHz/hPa [Rosenkranz, 1992; Bouazza *et al.* 1993]) and the atmospheric pressure profile, the 512 x 1 MHz spectrometer gives a frequency coverage wide enough to study O_3 abundances in relatively low atmospheric layers (above ~25 km), while the 256 x 100 kHz spectrometer gives a better frequency resolution in the central region of the line to study O_3 abundances in upper layers. Two reference absorbers at different temperatures (liquid N_2 and ambient) were used for calibration of the raw data in order to convert them to brightness temperature (total power observations). Most observations were carried out pointing the antenna close to the zenith. However, in a few cases, other elevation angles were used. This instrument has a half-power beam width (HPBW) of a few arcsec (depending on the frequency), so the effect of variation of the elevation along the beam can be completely neglected. It has been shown by de Zafra [1995] that this assumption can be kept for Gaussian beams up to 2^o of half width at half maximum when the observing angle is larger than 5^o or 6^o from the horizon.

The POM-2 instrument is a 2.5 m telescope located at Plateau de Bure in the French Alps, 2550 m above sea level [Castets *et al.*, 1988]. It is equipped with a

Table 2. General Information About Instruments Used During the Observational Work of Atmospheric Ozone Rotational Resonances

	Instrument	
Information	IRAM-30 m	POM-2
Latitude	37:04:05.60°N	44:38:02.00°N
Longitude	3:23:58.10°W	5:54:28.50°E
Altitude	2850 m	2550 m
Diameter	30 m	2.5 m
Operational frequencies	82-116 GHz 129-190 GHz 204-280 GHz 345-365 GHz	195-250 GHz
HPBW (230 GHz)	~12"	~2'
forward sky efficiency (η)	0.9	0.82
signal-image sideband ratio, G_S/G_I	4 for the 2 mm and 1.3 mm receivers 1 for the 355 GHz	1.3
η & G_S uncertainty	±3%	±5%
available spectrometers	512 x 1 MHz 256 x 100 kHz 1024 x 39 kHz	232 x 156 kHz 232 x 39 kHz

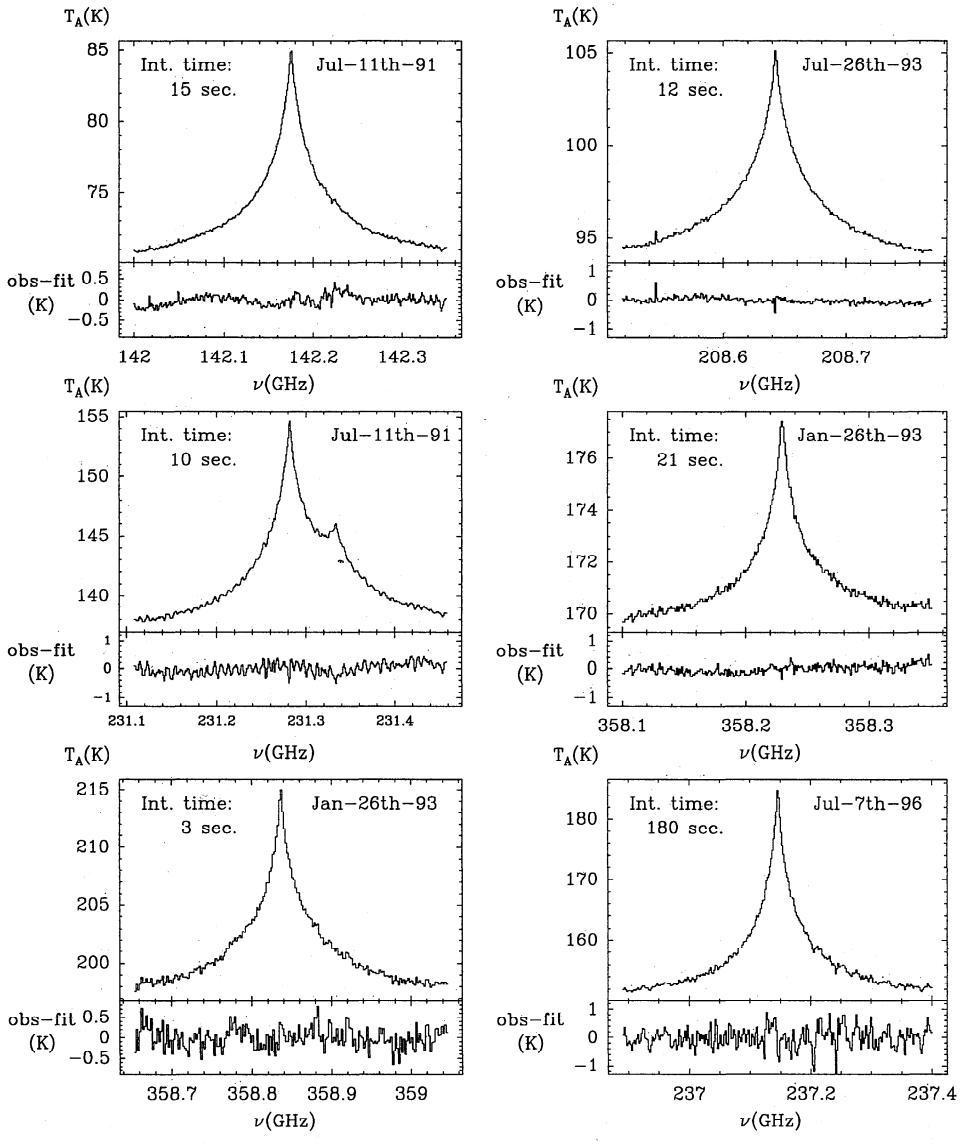

Figure 2. Examples of different O_3 atmospheric lines observed with the IRAM-30m telescope with the corresponding fit residual below. Derived O_3 mixing ratios with error bars from these and other observations can be found in Figure 5.

SIS receiver exhibiting a double-sideband (DSB) noise temperature $T_{receiver}$ of 65 ± 10 K. It operates in the frequency region from 195 to 250 GHz. Intermediate frequency ranges from 1.4 to 1.8 GHz and was selected for each observation individually in order to avoid the presence of atmospheric lines in the image sideband. The observations at POM-2 were always carried out at an elevation angle of 85^o (air mass = 1.004), with a half-power beam width (HPBW) of ~2'. A frequency switching procedure like the one described by Pardo et al. [1995] was used. The back-end spectrometer consists of an autocorrelator able to work at different resolutions from 156 kHz (total band of 36.25 MHz) to 39 kHz.

Figure 2 shows observations carried out at IRAM-30m and Figure 3 shows spectra obtained at POM-2. The residuals of the corresponding fits are given below each spectrum. They show that the instruments and the retrieval algorithm are working well at the different frequencies. We have to point out, however, that the residual of the 231.3 GHz spectrum in Figure 2 shows a sinusoidal behavior (probably due to standing waves), but it does not strongly affect the information about ozone retrieved from that particular spectrum. This work illustrates how the time devoted to calibration in astrophysical millimeter telescopes like the IRAM-30 m can be used to get interesting atmospheric data, the main intent of this work.

3. Inverse Radiative Transfer Algorithm

In the millimeter-wave range the solution of the radiative transfer equation, under the assumption of local thermodynamic equilibrium (LTE) and the Rayleigh-Jeans (R-J) approximation, can be written in terms of

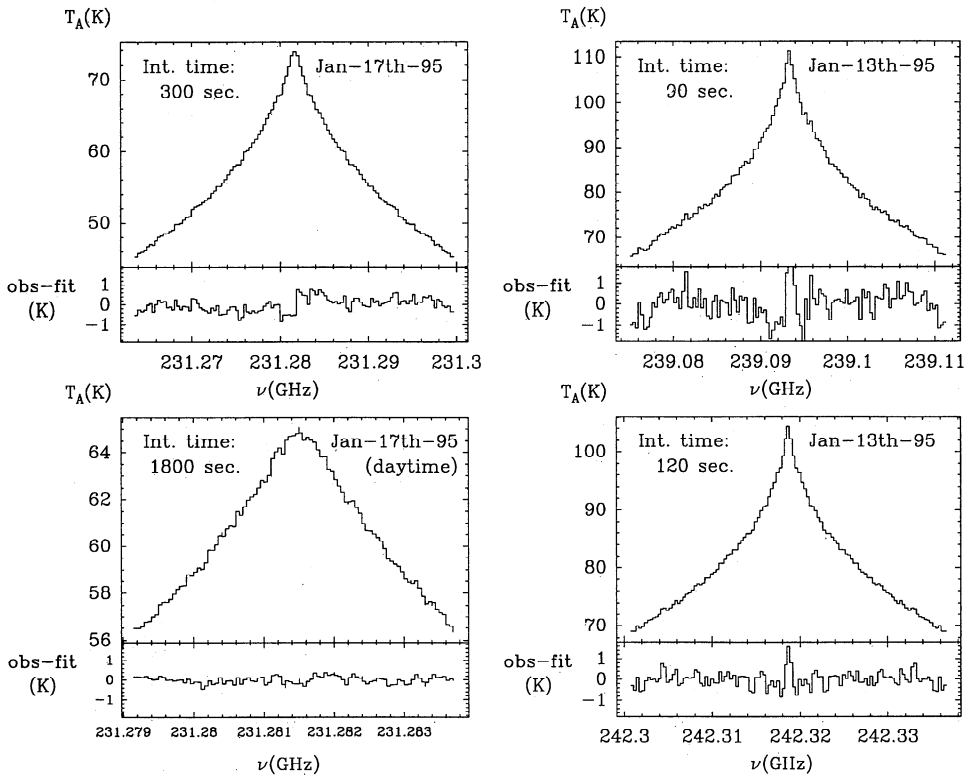

Figure 3. Examples of different O_3 atmospheric lines observed with the POM-2 telescope with the corresponding fit residual below. As for Figure 2, the derived O_3 mixing ratios with error bars from POM-2 observations are in Figure 5.

a brightness temperature [Chandrasekhar, 1960]:

$$T_{B\nu}(s) = T_{B\nu}(0)e^{-\tau_\nu(0,s)_\gamma} + \int_\gamma T(s')e^{-\tau_\nu(s',s)}\kappa_\nu(s')ds' \quad (1)$$

where s and s' are coordinates along the propagation path γ, and s=0 represents the initial boundary for γ. In the case of downward propagation to a ground-based detector, $T_{B\nu}(0)$ is essentially the cosmic background brightness temperature (if the telescope is pointing to a region of the sky without other external sources at frequency ν). The R-J expression at a given temperature loses validity with increasing frequencies, and in our case, it gives problems in treating the measurements we performed above 350 GHz (note that this approximation is based upon the fact $h\nu/kT \to 0$ but for ν=300 GHz and T=200 K, we get $h\nu/kT$=0.06). The more general equation is

$$kT_B(s) = \frac{h\nu}{e^{h\nu/KT_0}-1}e^{-\tau_\nu(0,s)} + \int_0^s \frac{h\nu}{e^{h\nu/KT}-1}e^{-\tau_\nu(s',s)}\kappa_\nu(s')ds' \quad (2)$$

where the R-J approximation to the Planck function (we are measuring thermal emission) has no longer been applied.

In the vicinity of a resonance frequency of a minor gas we can write almost exactly for the opacity $\tau_\nu = \tau_\nu(O_2)+\tau_\nu(H_2O)+\tau_\nu(\text{minor})$, and for the absorption coefficient $\kappa_\nu = \kappa_\nu(O_2)+ \kappa_\nu\ (H_2O)+\kappa_\nu(\text{minor})$. In principle, we need H_2O and temperature and pressure profiles as a priori information in order to perform the inversion. The inversion methods of Rodgers [1990] and Chahine-Twomey [Twomey, 1997] are based on a linearization of the problem. For example, in the R-J approximation those methods try to perform the inversion of

$$T_B(\nu) = T^*(\nu) + \int_\infty^{ground} W(\nu,s)N_{minor}(s)ds \quad (3)$$

where $T_B(\nu)$ are the measurements, $T^*(\nu)$ includes the preevaluated contribution of the cosmic background and the emission due to H_2O and O_2, $W(\nu,s)$ is called the minor constituent weighting function (this, in principle, can be also evaluated from a given a priori vertical profile of the constituent), and N_{minor} is the number density of the minor gas (the quantity searched for). From a set of measurements at n different frequencies, the atmosphere could be divided in m layers to obtain (from equation (3))

$$(T_B - T^*)_i = W_i^j N_{minor,j} \quad (4)$$

where i is associated to frequencies and j to layers. Thus the problem written in this manner appears linear in $N_{minor,j}$. Indeed, the strong correlation between the information coming from neighboring layers (cor-

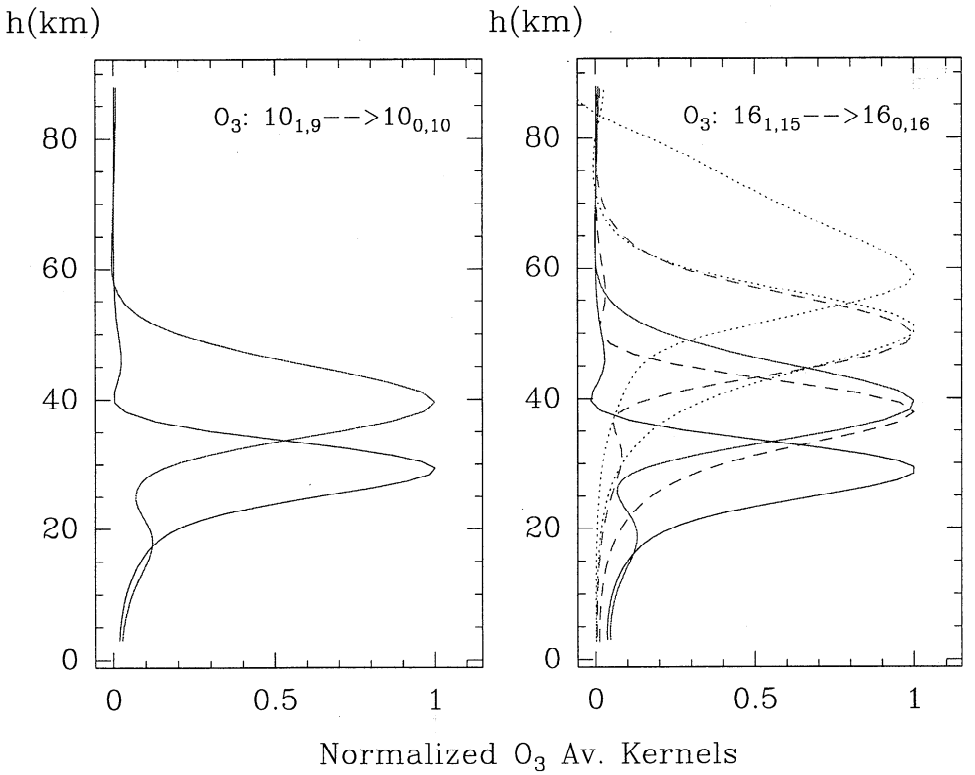

Figure 4. Examples of O_3 averaging kernels calculated during the pre-analysis described in the text and presented in Table 3. To the left we show the ones corresponding to the observation of the O_3 line centered at 142.17510 GHz using a 350 x 1 MHz spectrometer. To the right we show the same but for the 231.28151 GHz O_3 line observed with 350x1MHz (solid line), 116x312kHz (dashed line), and 232x39kHz (dotted line).

relation that appears in the rows of W_i^j) breaks down the uniqueness of the solution. Therefore the idea is to find a set of adjacent atmospheric layers from which information with low cross-correlation can be retrieved.

Our procedure for analyzing the data is as follows: we use the Backus-Gilbert method (cited in section 1) to set the location and vertical extent of the layers from which almost uncorrelated ozone mixing ratios can be retrieved, depending on the frequency coverage and resolution of the observation. We calculate for this goal a set of the so-called "averaging kernels" (see definition in references [Bevilacqua and Olivero, 1988; Pardo, 1996]). Examples of these calculations can be found in Figure 4. Second, we make radiative transfer calculations (using equation (1) or (2) and taking into account instrumental parameters; see below) and use a nonlinear least squares algorithm to fit the observation using as free parameters the ozone mixing ratios at the chosen layers as well as the integrated tropospheric water vapor amount. We take into account the ozone self-absorption near the line center. The a priori T-P profile is selected corresponding to the appropriate season and latitude of the observations (from the several profiles available on the U.S. Standard Atmosphere, 1976).

3.1. Adaptations for Instruments Used in This Work

The receivers on both radio telescopes were double sideband. Let T_{LSB} and T_{USB} be the brightness temperatures for the frequencies in the lower and upper sidebands, respectively (at frequencies where R-J is a good approximation). Then, the measured sky antenna temperature is [Cernicharo, 1988]:

$$T_{sky,meas} = T_{env} \cdot (1-\eta) + \eta[G_L T_{LSB} + G_U T_{USB}] \quad (5)$$

where η is the coupling coefficient between the antenna and the external sources (related to its radiation diagram $\eta \leq 1$); G_L and G_U are the relative gains of the lower and upper bands (G_L+G_U=1); and T_{env} is the ambient temperature. Our code takes into account the values of these instrumental parameters in order to finally give a synthetic spectrum to be compared with the measurements. In the following, the fit is achieved by means of a least square procedure which uses as free parameters ozone amounts in the layers selected by the Backus-Gilbert method cited above.

H_2O and O_2 absorption coefficients are taken from the model of Liebe *et al.* [1993]. For minor atmo-

Table 3. Preanalysis for Choosing Layers Where O_3 Mixing Ratios Will Be Relatively Uncorrelated During The Spectra Deconvolution Process

ν_c,(GHz) (Date/Telescope)	Spectrometer	Real Coverage	Layers km	Air Mass	Mixing Ratio Estimated Error, ±%[a]
142.17510 (July 1991/IRAM-30 m)	512 x 1 MHz	350 x 1 MHz	23.9-33.9	1.000	10.2
			33.9-46.2		11.3
142.17510 (July 1991/IRAM-30 m)	1024 x 39 kHz	944 x 39 kHz	31.6-43.0		5.8
			43.0-54.8	1.000	10.7
			54.8-70.0		11.5
208.64242 (July 1993/IRAM-30 m)	512 x 1 MHz	252 x 1 MHz	25.8-36.3	1.050	10.1
			36.3-48.6		7.9
231.28151+ 239.09326[b] (July 1991/IRAM-30 m)	512 x 1 MHz	350 x 1 MHz	23.3-33.6	1.000	5.6
			33.6-46.3		3.7
231.28151 (Jan. 1995/POM-2)	256 x 156 kHz	116 x 312 kHz	31.2-43.2	1.004	1.3
			43.2-57.0		3.6
231.28151 (July 1991/IRAM-30 m)	256 x 100 kHz	256 x 100 kHz	39.2-50.2	1.000	9.7
			50.2-62.7		10.6
231.28151 (Jan. 1995/POM-2)	256 x 39 kHz	232 x 39 kHz	42.4-57.5	1.004	4.0
			57.5-73.0		5.0
237.14613 (July 1996/IRAM-30 m)	512 x 1 MHz	256 x 2 MHz	23.9-33.9	1.773	4.1
			33.9-44.2		4.9
239.09326 (Jan. 1995/POM-2)	256 x 156 kHz	116 x 312 kHz	31.5-41.8	1.004	2.6
			41.8-56.5		3.8
242.31870 (Jan. 1995/POM-2)	256 x 156 kHz	116 x 312 kHz	31.4-42.8	1.004	1.7
			42.8-55.5		3.2
358.19981 (Jan. 1993/IRAM-30 m)	512 x 1 MHz	251 x 1 MHz	28.0-38.0	1.238	5.6
			38.0-48.5		5.0
358.85334 (Jan. 1993/IRAM-30 m)	512 x 1 MHz	256 x 2 MHz	25.7-33.5	1.495	6.2
			33.5-42.9		5.0

Total frequency coverage and frequency resolution are the key points for this choice.

[a]Estimated uncertainties for O_3 mixing ratios are given for 0.1 K Gaussian noise spectra (under the configuration given in the third column). A trade-off coefficient is used to weight the desired vertical resolution and the associated errors.

[b]This line appears in the spectrum via the image sideband.

spheric gases the line shape function we use is the Van Vleck-Weisskopf profile modified by Rosenkranz [1988] [see also Liebe, 1992; Liebe *et al.*, 1993]. This line shape is widely used to represent the pressure broadening mechanism that is completely dominant for minor atmospheric molecules in layers below ~60 km. From the references above, the pressure width parameter at ambient pressure P and temperature T can be written as

$$\Delta\nu_c = \Delta\nu_0(P/P_0)(T_0/T)^x \quad (6)$$

with respect to standard conditions P_0 and T_0 (usually 1013 hPa and 296 K). The typical values for $\Delta\nu_0$ and x of ~2-3 MHz/hPa and 0.5-1.2, respectively, for O_3 [see Gamache *et al.*, 1985; Rothman *et al.*, 1992; Rosenkranz, 1992; Bouazza *et al.*, 1993]. Since pressure varies much more quickly with the altitude than temperature, the effect of pressure is much more important in determining the line width. Doppler broadening, described by a Gaussian profile of the line shape, becomes important only for heights above $\simeq$ 60 km, where density is low enough. This broadening mechanism has been taken into account in order to carry out the inversion of high-resolution spectra (up to ~ 75 km). The Doppler broadening parameter for ozone is given by $\Delta\nu_D = 4.30x10^{-7}\nu_c(T/M)^{0.5}$ [Rosenkranz,

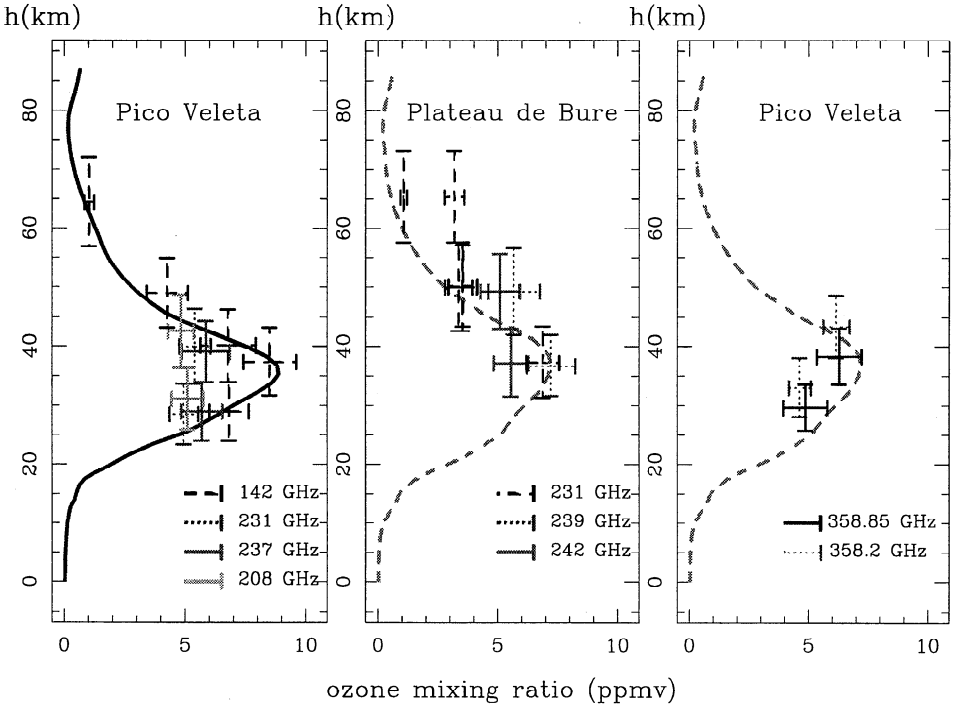

Figure 5. O_3 mixing ratios derived from ground-based observations of different rotational emission lines carried out with the IRAM-30 m and POM-2 radio telescopes. For the IRAM-30 m observations we have separated results from observations below 358 GHz which were all achieved in summertime (July) and from the first-time observed lines above 358 GHz in January 1993. Standard midlatitude summertime and wintertime O_3 mixing ratio vertical profiles are also plotted for comparisons.

1992], where M is the molecular weight of ozone. In the intermediate region (~40 to 65 km) where the two broadening mechanisms are competitive, the analysis has taken into account a convolution of both line shapes resulting in a Voigt line profile. We use the pressure-broadening coefficient and temperature exponent given by Rosenkranz (1992) from laboratory experiments of collisions between O_3-N_2 and O_3-O_2. They can also be found in Table 1.

Here we present analysis of only O_3 spectroscopic observations, but the first ground-based observations of middle atmospheric water vapor from the ground using the 183.31 GHz resonance have been analyzed similarly in a preceding paper [Pardo *et al.*, 1996].

4. Analysis of O_3 Observations

Table 3 shows the layers where the O_3 mixing ratios are considered as free parameters for deconvolution of the different observations. These layers have been selected after a pre-analysis based on the Backus-Gilbert method [see Pardo et al., 1996]. The instrumental parameters taken into account for the inversion process can be found in Table 2.

Figures 2 and 3 show some observations and their corresponding fits achieved by our inversion code. The retrieved O_3 mixing ratios for those and other observations are given in Figure 5, where they are compared with standard O_3 vertical profiles for the season and the latitude zone of the observations (as given in the U.S. Standard Atmosphere, 1976).

Uncertainties in the retrieved mixing ratios come from data noise (including baseline quality), assumed a priori information (both atmospheric information and spectroscopic data such as line strength and broadening parameters) and instrumental parameters. We have checked and estimated the errors coming from each one of these possible sources.

4.1. Errors From Temperature and Pressure a Priori Information

In the present case, we do not have simultaneous O_3 spectroscopic measurements and $T-P$ vertical profiles measurements. Therefore we take a standard $T-P$ profile according to the place and season of the observation (from the U.S. Standard Atmosphere, 1976) in order to analyze the O_3 data. To check the uncertainties that this assumption introduces, we use $T-P$ profiles as a priori information which are different with respect to a $T-P$ reference profile. For example, for an observation carried out at Pico Veleta during the winter season, we use as reference the U.S. Standard Atmosphere, 1976, type 3 (midlatitude winter), and we compare the results with those obtained when using a different $T-P$ information, for example, U.S. Standard Atmosphere 1976, types 2 and 4 (midlatitude summer and subarctic summer). Since the difference between the real $T-P$ profile during the observations and the reference is ex-

Table 4. Relative Errors (in percent) on Calculated O_3 Mixing Ratios From Observations Reported in This Paper.

			Relative Errors, ±%				
ν_c,	Spectrometer	Layers	A Priori	Data[a]	Instrumental		Root Sum
GHz	(Real Coverage)	km	Atm. Profile	Noise	η	G_S	Square Error
142.17510	512x1MHz	23.9-33.9	4	11	1	3.5	12
	(350x1MHz)	33.9-46.2	10	13	1	3.5	17
142.17510	1024x39kHz	31.6-43.0	8	9	1	4	13
	(944x39kHz)	43.0-54.8	10	17	1	3	20
		54.8-70.0	8	18	1	4	20
208.64242	512x1MHz	25.8-36.3	5	11	0.5	5	13
	(252x1MHz)	36.3-48.6	7	8	0.5	3	11
231.28151	512x1MHz	23.3-33.6	4	11	1	2	12
+ 239.09326	(350x1MHz)	33.6-46.6	8	7	1	6	12
231.28151	256x156kHz	31.2-43.2	6	4		7	10
	(116x312kHz)	43.2-57.0	9	12		8	17
231.28151	256x100kHz	39.2-50.2	10	10	1	6	15
	(256x100kHz)	50.2-62.7	8	17	1	2	19
231.28151	256x39kHz	42.4-57.5	13	7		8	17
	(232x39kHz)	57.5-73.0	6	9		7	13
237.14613	512x1MHz	23.9-33.9	10	11	1	3.5	15
	(256x2MHz)	33.9-44.2	12	12	1	3.5	17
239.09326	256x156kHz	31.5-41.8	5	10		8	14
	(116x312kHz)	41.8-56.5	9	15		8	19
242.31870	256x156kHz	31.4-42.8	8	6		9	13
	(116x312kHz)	42.8-55.5	8	12		8	16
358.19981	512x1MHz	28.0-38.0	4	8	2	5	10
	(251x1MHz)	38.0-48.5	3	7	2	4	9
358.85334	512x1MHz	25.7-33.5	6	16	4	6	19
	(256x2MHz)	33.5-42.9	4	13	3	5	15

[a]The estimations given in this column come from the analysis presented on Table 3 taking into account the mean value of the spectra noise.

pected to much smaller than the difference between U.S. Standard Atmosphere, 1976, types 2 and 4 to the reference, we multiply the obtained partial error-bar by 0.5. Detailed values of the derived uncertainties can be found in Table 4. The shape of the tropospheric water vapor distribution (assumed exponentially decreasing) is a less important source of uncertainty because the integrated tropospheric contribution to the absorption of the stratospheric signal is very smooth in the frequency range of the obtained spectra (the observed lines are far from H_2O resonances). Using different distributions of the tropospheric water vapor for the same total amount, we estimate the uncertainty on the tropospheric transmission through the passbands used in the observations to be less than 4%. Thus to determine the emission level above which the O_3 line appears, we only use the integrated tropospheric water vapor amount as a free parameter of the least squares procedure (assuming a scale height of 2 km), rather than its detailed vertical distribution.

4.2. Errors From Data Noise

Data noise introduces an error in these kinds O_3 mixing ratios derived from this kind of spectroscopic observation. In fact, there is a trade-off between the importance of these errors and the vertical resolution desired from the deconvolution algorithms. The Backus-Gilbert method quantifies this trade-off. For a particular choice of layers in the deconvolution process it is possible to

estimate these errors (for a given data noise). In Table 4 we give the corresponding estimated values of these errors for the observations we present in this paper (typical noise level between 0.1 and 0.3 K) taking into account our choice of layers for individual deconvolution, based on the preanalysis presented in section 3.

4.3. Errors From the Instrumental Parameters

These errors are known as "calibration errors." Assuming that the two absorbers used as blackbodies for this purpose have enough temperature stability, the error will mainly come from the uncertainties in the coupling coefficient η and the sideband gain ratio (see equation (5)). Uncertainty in the knowledge of these parameters is estimated to be $\sim \pm 3\%$ for the IRAM-30 m telescope and $\sim \pm 5\%$ for POM-2. In order to check their effect on the retrieved O_3 amounts we have carried out the inversion for a set of values of η and G_S within the uncertainty range around the assumed values (given in Table 2). The errors given in the corresponding column of Table 4 are the mean of several tests on the range limits. Assuming no systematic error sources, we determine the total error bars given in Table 4 and shown in Figure 5 by root-sum-square of errors coming from individual sources.

5. Discussion: Some Particular Results

The whole set of spectra (examples in Figures 2 and 3) gives information on the ozone abundance over a wide altitude range (from 25 to 72.5 km as extreme values, corresponding to the best frequency coverage and to the best frequency resolution respectively) for winter and summer in southern Europe over several years. This is a limited data set because it does not belong to a systematic O_3-monitoring program, but the data are interesting in order to show the feasibility of these kinds of measurements using different O_3 lines. The data from observations of different lines show good consistency. Our careful analysis has allowed us to compare the results coming from different frequencies and telescopes.

Most of our observations have been achieved above 200 GHz, whereas most ground-based radiometers for O_3 monitoring work at frequencies below 150 GHz. Avoiding the problem of higher tropospheric opacity in the region 200-300 GHz by placing the receiver at high mountain sites, some of the ozone lines in this range are better suited to study ozone profiles than those below 150 GHz due to their intrinsic stronger intensity (some of them, on the other hand, have the drawback of being weaker or relatively more temperature sensitive; see below the case of the 358.2 GHz resonance). We have made radiative transfer calculations to compare the expected brightness temperatures at Pico Veleta (zenith view) for the frequencies of the eight O_3 lines presented in this work using the same atmospheric profile: U.S. Standard, 1976, midlatitude winter with 1.8 mm of precipitable water vapor above 2.9 km (typical winter time conditions on the site). The results of such calculations are shown in Figure 6 to give an idea of expected relative intensities. The atmospheric conditions used in the simulations give an atmospheric opacity at 225 GHz of 0.131. Opacities equal or lower than that happen during an important part of the winter season in Pico Veleta [see Pardo, 1996]. The calculations show that the difference between the T_B at the peak and the continuum is around twice larger for the 231, 237, 239, 242, and 358.8 GHz lines with regard to the 142, 208, and 358.2 GHz lines.

Three to five receivers can be used simultaneously at the IRAM-30 m telescope. We want to point out the possibility of simultaneous observations of several O_3 lines. This could allow a simultaneous inversion with the code presented here, improving the reliability of the

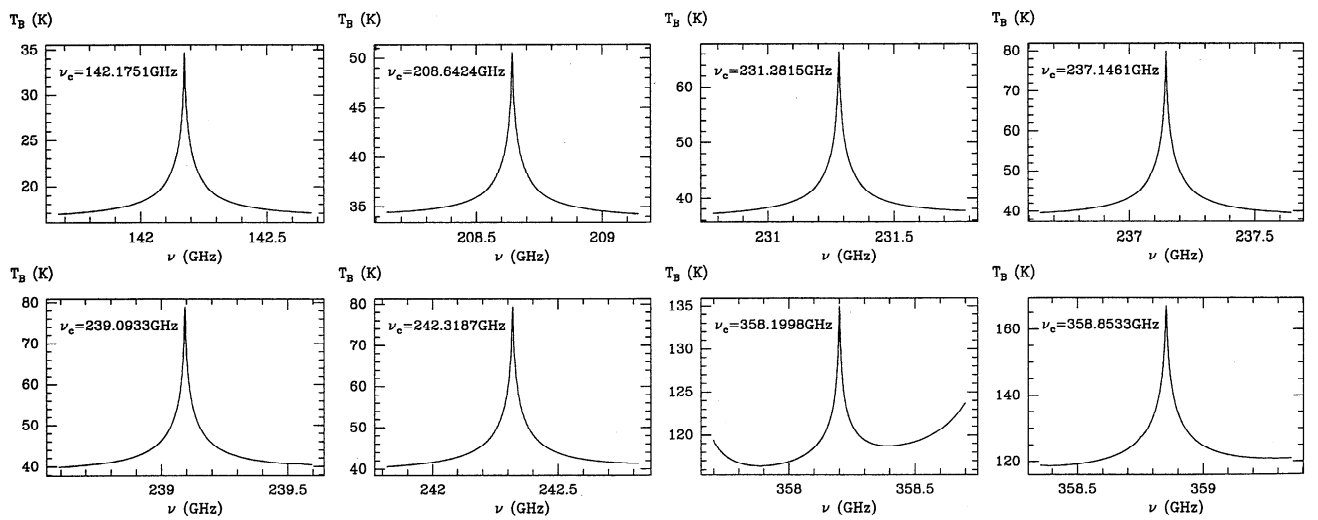

Figure 6. Radiative transfer simulations of the eight O_3 lines we have observed in order to compare their expected T_B (according to equation (2)) under the same atmospheric conditions: U.S. Standard, 1976 midlatitude winter, 1.8 mm precipitable water, observing point at 2.9 km above sea level and zenith view (a typical during winter at the site of the IRAM-30 m telescope).

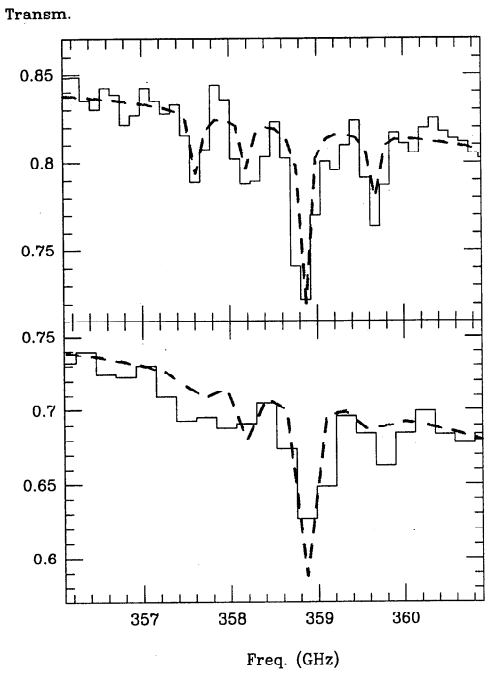

Figure 7. Data (histogram) on the atmospheric transmission taken with an FTS spectrometer on the CSO telescope (4.1 km above sea level on Mauna Kea, Hawaii). The data actually extend from 170 to 980 GHz. We show here the region 356-361 GHz with the two ozone lines above 358 GHz we observed at Pico Veleta. The dashed line is the fit achieved on the basis of our ATM forward model. Observations were performed in clear sky conditions with 0.7 mm of estimated water amount above the telescope and air mass = 1 for the top part of the figure and 0.95 mm and air mass = 1.4 for the bottom part (~3 times less frequency resolution).

results due to a lesser dependence upon the instrumental errors.

From the observational point of view, one of the original reasons for our work has been the good quality spectra obtained above 358 GHz at Pico Veleta in January 1993. Of the two observed lines (358.2 and 358.85 GHz), the one at higher frequency is expected to present stronger emission due to its much lower excitation temperature (despite a weaker line strength). Confirmation of this point is given by our model calculations and also from the good data (despite an overestimation of the line width due to instrumental effects) obtained by Serabyn *et al.* [1997] (see Figure 7). As a result, it is possible to start at lower altitudes and to retrieve better O_3 information from the 358.85 GHz line than from the 358.2 GHz transition when using the same frequency coverage (see Table 3). The O_3 retrievals using the second line (higher excitation temperature) have, in addition, an important additional uncertainty due to the lack of information about the true stratospheric temperature. In fact, this is on the ground of the poor agreement between the 358.2 GHz data and the 358.8 GHz data in Figure 5.

5.1. Diurnal [O_3] Variation Above ~55 km

Although the data described in this paper do not represent an extensive O_3-monitoring campaign, we performed, during a week in January 1995, repeated observations of the central region of the 231.281 GHz ozone line. Observations were carried out twice per 24 hours (once at nighttime and once at daytime) using a frequency resolution of 39 KHz. Significant differences between nighttime and daytime ozone abundances are

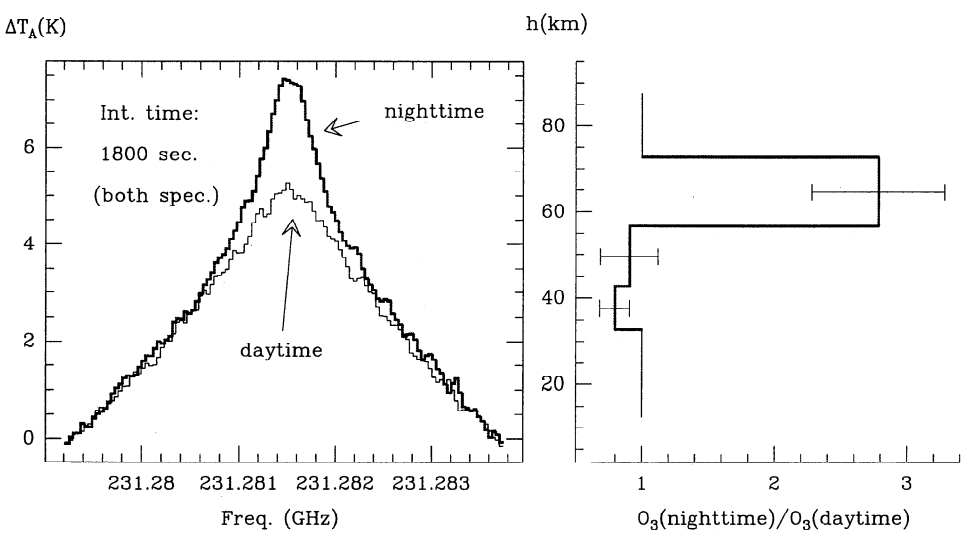

Figure 8. Comparison of two O_3 observations at 231.282 GHz carried out at the same elevation during nighttime and daytime. We show also the mean ratio between the retrieved O_3 amounts during nighttime and daytime, in the layers considered, corresponding to the whole set of observations carried out in January 1995 at Plateau de Bure. At the central frequencies, most of the signal comes from layers where the Doppler broadening mechanism becomes comparable or even dominant with respect to the pressure broadening (we take this into account in the analysis by introducing a convolution of the Van Vleck-Weisskopf line shape and the Doppler line shape resulting in a Voigt profile). The O_3 amounts in the layer 32.5-42.5 km were derived from complementary observations carried out with the 232 x 156 kHz mode of the autocorrelator.

expected for stratomesospheric altitudes (above 50 km) from models [Vaughan,1984; Prather, 1981] and previous measurements: Wilson and Schwartz [1981], the first people to report on this effect, Lobsiger and Künzi [1986], and Zommerfelds *et al.* (1989], who used a set of 31 filter channels with a frequency resolution increasing from the line wings (30 MHz) to the line center (0.2 MHz) to observe the 142.175 ozone resonance; Ricaud *et al.* [1991] reported on measurements of the 110.836 O_3 line with a 256 x 100 kHz filter bank; Tsou *et al.* [1995] had a frequency resolution of 50 kHz near the 110.836 GHz O_3 resonance. We report in this paper the measurements of daytime-nighttime O_3 number density ratios over Plateau de Bure with a high-frequency resolution (39 kHz) and the highest observing frequency to spectral resolution ratio.

Figure 8 shows the comparison between a nighttime and a daytime observation carried out at the same elevation with the same integration time. The increase of mesospheric ozone emission at nighttime is clearly seen. Relative values of ozone abundances at nighttime and daytime in the layers given in Table 3 are also shown in the same figure. Results show an abundance ~2.5 times higher during nighttime than during daytime in the layer 56.5-72.5 km. These results are in agreement with the recent measurements by Kawabata *et al.* [1997] and also with results by Ricaud *et al.* [1991], Connor *et al.* [1994], and Tsou *et al.* [1995], and with previous 0-D models [e.g., Ricaud *et al.*, 1994]. No clear differences above the retrieval uncertainty are seen in the lower layers, as expected also from model calculations [Ricaud *et al.*, 1994] and confirmed by the measurements cited just above. We point out that our results seem to confirm a ratio (nighttime/daytime) of O_3 abundances below 1 for the layer 32.5-42.5 km, a tentative result found by Kawabata *et al.* [1997] and Connor *et al.* [1994] at 3.2 hPa (~40 km of altitude).

5.2. Ozone in the Lower Stratosphere Ozone Over Pico Veleta

For some of our observations we used a wide spectrometer (0.512 GHz of frequency coverage) in order to take high-quality spectra of some O_3 millimeter lines (Figures 2 and 3). As we show in Table 3, such a frequency coverage allows us to obtain information about ozone above ~25 km, thereby probing the layers where the bulk of atmospheric ozone is located. Other ground-based millimeter-wave measurements have reported ozone data below 30 km (see Tsou et al. [1995], Peter and Kämpfer [1995] who have measured down to 15 km with 1.2 GHz bandwidth using the 142.175 GHz ozone line [Cheng et al., 1996, 1997]).

Table 5 gives O_3 concentrations measured in the lower stratosphere over Pico Veleta in the summer of 1991 and 1993. The vertical extent of the layer depends on the effective frequency coverage retained for the inversion, as we said in section 4. The measurements at 142 and 231 GHz carried out on the same date show a good consistency within the error bars. We infer from these observations O_3 amounts close to standard values over this site.

6. Summary and Conclusions

We have good-quality ground-based spectroscopic observations of several rotational lines of atmospheric O_3 in the frequency range 142 to 359 GHz. Two different ground-based radio telescopes in Southern Europe have been used for this work in several periods from 1991 to 1996. The observations have been fitted by means of a generalized least squares procedure based on the forward radiative transfer model (ATM), described by Pardo [1996], in order to retrieve O_3 mixing ratios at different altitudes.

Table 5. O_3 Amounts in the Lower Stratosphere in Southern Spain Derived From Observations Carried Out With the IRAM-30 m Telescope Using a 512 x 1 MHz Spectrometer

ν_c, GHz	Date	Layer, km	$\overline{\rho_{O_3}}(\mathrm{cm}^{-3})$ -Error Bar- (stand. atm.)
142.17510	July 11, 1991.	23.9-33.9 km	3.8-5.0 x 10^{12} (3.07×10^{12})
231.28151	July 11, 1991.	23.3-33.6 km	3.0-3.9 x 10^{12} (3.10×10^{12})
358.19981	Jan. 27, 1993.	28.0-38.0 km	1.2-1.6 x 10^{12} (1.82×10^{12})
358.85334	Jan. 27, 1993.	25.7-33.5 km	3.0-6.0 x 10^{12} (2.67×10^{12})
208.64242	July 26, 1993.	25.8-36.3 km	1.9-2.8 x 10^{12} (2.77×10^{12})
237.14613	July 7, 1996.	23.9-33.9	2.8-3.9 x 10^{12} (2.97×10^{12})

This work is a good test for our retrieval algorithm because it has been applied to observations coming from different telescopes, using different backends and over a wide range of frequencies (142 to 359 GHz). The algorithm worked well in all cases, and the results were consistent (within the error bars) for different O_3 lines observed the same day with the same instrument. An analysis of the errors coming from the usual sources in these kinds of retrievals (e.g., data noise, instrumental parameter uncertainties, T-P information) has been performed. The results of this analysis show that the uncertainties on the retrieved O_3 mixing ratios do not exceed $\pm 20\%$ in any case and are less than $\pm 16\%$ in most of them.

Among the data presented in this paper some are of special interest: first, the observations at 142, 208, 231, and 358 GHz with a wide frequency coverage (a 512 x 1 MHz spectrometer was used) which allow the study of ozone in relatively low layers (above $\sim$ 25 km). On the other hand, we have done observations at high-frequency resolution (39 kHz) of the central region (4 MHz of frequency coverage) of the 231.282 GHz ozone line (Figure 3). These observations allow retrieval of ozone abundances up to $\sim$72 km and clearly show the diurnal cycle of ozone abundance in the mesosphere. Finally, in this work we have reported O_3 mixing ratio retrievals for the first time on ground-based measurements of two O_3 lines located above 358 GHz which provide material for planning of future stratospheric ozone monitoring.

Acknowledgments. J.R. Pardo gratefully acknowledges the financial support of the Observatoire de Paris-Meudon and the use of its facilities during the development of this work. He specially thanks C. Prigent, G. Beaudin, P. Encrenaz and Y. Viala for guiding his work in France. He also recognizes the NASA Goddard Institute for Space Studies for supplying him with computer facilities during the final phase of this work. We also thank the Observatoire de Grenoble and IRAM for allowing us the use of the POM-2 and IRAM-30 m radio telescopes respectively, and for financial support during the observations. His work has also been partially supported by the Spanish CICYT, under project PB93-0048. José Cernicharo thanks the DGES for support through ACP96-0168 and ESP96-2529-E.

References

Backus, G., and F. Gilbert, Uniqueness in the inversion of inaccurate gross Earth data, *Philos. Trans. R. Soc. London,* 266, 123-192, 1970.

Bevilacqua, R. M., W.J. Wilson, and P.R. Schwartz, Measurements of mesospheric water vapor in 1984 and 1985: Results and implications for middle atmospheric transport, *J. Geophys. Res.,* 92, 6679-6690, 1987.

Bevilacqua, R. M., and J.J. Olivero, Vertical resolution of middle atmospheric measurements by ground-based microwave radiometry, *J. Geophys. Res.,* 93, 9463-9475, 1988.

Bouazza, S., A. Barbe, J.J. Plateaux, L. Rosenmann, J.M. Hartmann, C. Camy-Peyret, J.M. Flaud, and R.R. Gamache, Measurements and calculations of room-temperature ozone line-broadening by N_2 and O_2 in the $\nu_1+\nu_3$ band, *J. Mol. Spectrosc.,* 157, 271-289, 1993.

Castets, A., et al., The 2.5-m millimeter telescope on Plateau de Bure, *Astron. Astrophys.*, 194, 340-343, 1988.

Cernicharo, J., *Thèse de Doctorat d'État,* Univ. de Paris VII, 1988.

Chandrasekhar, S., Radiative Transfer, Dover Publications, Inc., N.Y., 1960.

Cheng, D., R.L. de Zafra, and C. Trimble, Millimeter wave spectroscopic measurements over the south pole, 2, An 11-month cycle of stratospheric ozone observations during 1993-1994, *J. Geophys. Res.,* 101, 6781-6793, 1996.

Cheng, D., R.L. de Zafra, and C. Trimble, Millimeter wave spectroscopic measurements over the south pole, 4, O_3 and N_2O during 1995 and their correlations for two quasi-annual cycles, *J. Geophys. Res.,* 102, 6109-6116, 1997.

Connor B.J., D.E Siskind, J.J. Tsou, A. Parrish, and E.E. Remsberg, Ground-based microwave observations of ozone in the upper stratosphere and mesosphere, *J. Geophys. Res.,* 99, 16,757-16,770, 1994.

de Zafra, R.L., J.M. Reeves, and D.T. Shindell, Chlorine monoxide in the Antarctic spring vortex, 1, Evolution of midday vertical profiles over McMurdo Station in 1993, *J. Geophys. Res.,* 100, 13,999-14,007, 1995.

de Zafra, R.L., Ground-based measurements of stratospheric trace gases using quantitative millimeter wave emission spectroscopy, in Diagnostic Tools in Atmospheric Physics, IOS Press, Amsterdam, 1995.

Gamache, R.R., and L.S. Rothman, Theoretical N_2-broadened half-widths of $^{16}O_3$, *Appl. Opt.,* 24, 1651-1655, 1985.

Gordy, W., and Cook, R.L., *Microwave Molecular Spectra,* John Wiley, New York, 1984.

Kawabata, K., H. Ogawa, Y. Yonekura, H. Suzuki, M. Suzuki, Y. Iwasaka, K. Shibata, and T. Sakai, *J. Geophys. Res.,* 102, 1371-1377, 1997.

Liebe, H.J., Models for refractive index of the neutral atmosphere at frequencies below 1000 GHz, in Physics of the Upper Atmosphere, edited by W. Dieminger et al., Springer-Verlag, New York, 1992.

Liebe, H.J., G.A. Hufford, and M.G. Cotton, Propagation modeling of moist air and suspended water/ice particles at frequencies below 1000 GHz, in proceedings of Advisor Group Aerosp. Res. and Dev., NATO, Brussels, 52nd Specialists' Meeting of the Electromagnetic Wave Propagation Panel, 1993.

Lobsiger, E., and K.F. Künzi, Nighttime increase of mesospheric ozone measured with ground-based microwave radiometry, *J. Atmos. Sol. Terr. Phys.,* 48, 1153-1158, 1986.

Nedoluha, G.E., R.M. Bevilacqua, R.M. Gomez, D.L. Thacker W.B. Waltman, and T.A. Pauls, Ground-based measurements of water vapor in the middle atmosphere, *J. Geophys. Res.,*, 100, 2927-2939, 1995.

Pardo, J.R., Thèse de Doctorat: "Etudes de l'atmosphère terrestre au moyen d'observations dans les longueurs d'onde millimétriques et submillimétriques", Univ. Pierre et Marie Curie (Paris VI) - Univ. Complutense de Madrid, 1996.

Pardo, J.R., L. Pagani, M. Gerin, and C. Prigent, Evidence of the Zeeman splitting in the $2_1 \rightarrow 0_1$ rotational transition of the atmospheric $^{16}O^{18}O$ molecule from ground-based measurements, *J. Quant. Spectrosc. Radiat. Transfer,* 54 (N6), 931-943, 1995.

Pardo, J.R., J. Cernicharo, E. Lellouch, and G. Paubert, Ground-based measurements of middle atmospheric water vapor at 183 GHz during very dry tropospheric conditions, *J. Geophys. Res.,* 101, 28,723-28,730, 1996.

Peter, R., and N. Kämpfer, Short-term variations of mid-latitude ozone profiles from ground based millimetric wave observations during the winter 1994/95, paper presented at the third European Workshop on Polar Stratospheric Ozone, Schliersee, Germany, September 1995.

Prather, M.J., Ozone in the upper stratosphere and mesosphere, *J. Geophys. Res.*, 86, 5325-5338, 1981.

Ricaud, P., J. Brillet, J. de La Noë, and J.P. Parisot, Diurnal and seasonal variations of strato-mesospheric ozone: Analysis of ground-based microwave measurements in Bordeaux, France, *J. Geophys. Res.*, 96, 18,617-18,629, 1991.

Ricaud, P., G. Brasseur, J. Brillet, J. de La Noë, J.P. Parisot and M. Pirre, Theoretical validation of ground-based microwave ozone observations, *Ann. Geophys.*, 12, 664-673, 1994.

Rodgers, C.D., The vertical resolution of remotely sounded temperature profiles with a priori statistics, *J. Geophys. Res.*, 95, 5587-5595, 1990.

Rosenkranz, P.W., Interference coefficients for overlapping oxygen lines in air, *J. Quant. Spectrosc. Radiat. Transfer* 39, 287-297, 1988.

Rosenkranz, P.W., Appendix to chapter 2, in Atmospheric Remote Sensing By Microwave Radiometry, edited by M.A. Janssen, Wiley-Interscience, New York, 1992.

Rothman, L.S., et al., The HITRAN molecular database: Editions of 1991 and 1992, *J. Quant. Spectrosc. Radiat. Transfer*, 48, 469-507, 1992.

Serabyn, E., E.W. Weisstein, D.C. Lis, and J.R. Pardo, Submillimeter FTS measurements of atmospheric opacity above Mauna Kea, *Appl. Opt.*, in press, 1998.

Tsou, J.J., J.J. Olivero, and C.L. Croskey, Study of variability of mesospheric H_2O during spring 1984 by ground-based microwave radiometric observations, *J. Geophys. Res.*, 93, 5255-5266, 1988.

Tsou, J.J., B.J. Connor, A. Parrish, I.S. McDermid, and W.P. Chu, Ground-based microwave monitoring of middle atmosphere ozone: Comparison to lidar and Stratospheric and Gas Experiment II satellite observations, *J. Geophys. Res.*, 100, 3005-1016, 1995.

Twomey S.S., Introduction to the Mathematics of Inversion in Remote Sensing and Indirect Measurements, Elsevier, New York, 1997.

Vaughan, G., Mesospheric ozone: Theory and observation, *Q. J. R. Meteorol. Soc.*, 110, 239-260, 1984.

Wilson, W.J., and P.R. Schwartz, Diurnal variations of mesospheric ozone using millimeter-wave measurements, *J. Geophys. Res.*, 86, 7385-7388, 1981.

Zommerfelds, W.C., K. Künzi, M.E. Summers, R.M. Bevilacqua, D.F. Strobel, M. Allen, and W.J. Sawchuk, Diurnal variations of mesospheric ozone obtained by ground-based microwave radiometry, *J. Geophys. Res.*, 94, 12,819-12,832, 1989.

J. R. Pardo, NASA-Goddard Institute for Space Studies, 2880 Broadway, New York, NY 10025, USA. (e-mail: jpardo@giss.nasa.gov).

J. Cernicharo, CSIC, IEM, Departamento de Física Molecular, Serrano 123, E-28006 Madrid, Spain. (e-mail: cerni@astro.iem.csic.es).

L. Pagani, DEMIRM, URA336 du CNRS, Observatoire de Paris-Meudon, 61 Avenue de l'Observatoire, 75014 Paris, France. (e-mail: pagani@mesioa.obspm.fr).

(Received May 7, 1997; revised December 4, 1997; accepted December 11, 1997.)